J Mater Sci (2007) 42:4260–4264
DOI 10.1007/s10853-006-0638-y

Effect of structure change on thermal and dielectric characteristics in low-temperature firing Bi_2O_3–B_2O_3–ZnO glasses

Byung-Sook Kim · Eun-Sub Lim · Joon-Hyung Lee · Jeong-Joo Kim

Received: 16 August 2005 / Accepted: 5 July 2006 / Published online: 28 February 2007

Abstract In a Bi_2O_3–B_2O_3–ZnO glass system, glass structure change, sintering behavior and resultant physical characteristics of the glass were examined when various amounts of Bi_2O_3 and ZnO mixture were added. When the total amount of Bi_2O_3 and ZnO was below 30 mol%, a phase separation occurred and homogeneous glass was not obtained. The fraction of four-coordinated borons (BO_4) was highest when the total amount of Bi_2O_3 and ZnO was 50mol%. Further addition over 50 mol% induced a borate anomaly phenomenon in the glass, which resulted in the decrease in BO_4 fraction. The sintering temperature and glass transition temperature decreased as the amount of Bi_2O_3 and ZnO increased. The thermal expansion coefficient and dielectric constant of the specimens were also examined.

Introduction

In the borate glasses, which are composed of a basic unit of two dimensional BO_3 triangles, the aggregates of three such triangles form the B_3O_6 boroxol groups, which in turn form an irregular network [1]. When a network modifier is added, the incorporation of alkali oxides lead to a coordination shift from three-coordinated (BO_3) to four-coordinated borons (BO_4) with alkali ions adjoining the BO_4 tetrahedron. Further addition over the point where the highest BO_4 fraction is obtained, results in a retrograde coordination shift from BO_4 to BO_3. The glass structure changes with variations of the composition are referred to as the borate anomaly [2, 3]. The structural change is known to affect the physical characteristics of the glasses such as glass transition temperature, thermal expansion temperature and density [4, 5]. The borate anomaly has been examined in various glass systems particularly from the view point of the N_4 value, which determines the maximum fraction of boron atoms in the BO_4 structure out of total number of boron atoms in a glass [6–12].

In two component alkali borate glasses, Bray [6] found the maximum amount of alkali oxide (N_4) to be around 40 mol%, which was analyzed by the nuclear magnetic resonance (NMR) technique. The alkaline earth borate glass system also showed the N_4 value around 40 mol% of alkaline earth oxides [7]. The ionic field strength of alkali and alkaline earth oxides, which play the role of network modifiers in B_2O_3, is around 0.1–0.2 and 0.2–0.5, respectively, and most of the added oxides form four-coordinated borons [2, 6].

On the other hand, PbO [8, 9], SnO [10], CdO [11] and ZnO [12], which exhibit ionic field strength around 0.5–1.0 and which play the role of intermediates in B_2O_3, the N_4 value for those oxides was around 50 mol% in two component borate glasses. Bray [9] explained that the larger N_4 values in PbO–B_2O_3 glass than in alkali borate glass are due to the fact that PbO works not only as modifier Pb^{2+} ions to form BO_4 units but also as a former to enter the glass network as B_3–O–Pb linkages. The maximum composition of N_4 value for CdO and ZnO also increased to 50 mol% because they played the role of network formers too [11]. In the

---

B.-S. Kim · E.-S. Lim · J.-H. Lee · J.-J. Kim (✉)
Department of Inorganic Materials Engineering,
Kyungpook National University, Daegu 702-701, Korea
e-mail: jjkim@knu.ac.kr

case of SnO, N_4 also increased since all the added SnO is not only used to form the BO_4 units but also used to form NBO (B–O···Sn) in a composition range with lower SnO contents [10].

In this study, two kinds of oxides of Bi_2O_3 and ZnO, which have ionic field strengths of 0.5–1, were selected because they were expected to play the role of intermediaties. Bi_2O_3 and ZnO were mixed at a 1:1 ratio and added to the B_2O_3. The formation of the BO_4 structure, the sintering behavior of the glass, the thermal expansion coefficient, the glass transition temperature and the dielectric characteristics of the sintered glass were examined as a function of the amount of Bi_2O_3 and ZnO.

Experimental procedure

Compositions of the glasses in this experiment are xBi_2O_3–xZnO-$(1-2x)B_2O_3$, where $x = 0.15$, 0.20, 0.25, 0.30, 0.35, and 0.40. High purity chemicals of Bi_2O_3 (Kojundo chemical lab co., Ltd, 99.6%, Japan), H_3BO_3 (Kojundo chemical lab co., Ltd, 99.9%, Japan), and ZnO (Aldrich, 99.9%, U.S.A) were used as starting raw materials. Weighed raw powders were mixed in an alumina crucible for 15 min, and melted at 1,100°C for 30 min in a Pt crucible. The molten glass in the crucible was dropped into cold water for quenching. The glass frit was roughly crushed in an alumina mortar and then Planetary-milled for 2 h at 400 rpm. The glass powders were analyzed using an X-ray diffractometer (MO3-XHF, MAC Science Co., Japan). The structure of the glass was examined using a 600 MHz Solid-State NMR Spectrometer (Unity INOVA600, Varian) on the basis of ^{11}B NMR analysis. The glass transition temperature was measured using a DSC (Thermal Analyzer, DSC 2920, TA Instruments, U.S.A.).

The glass powders were isostatically pressed under a pressure of 100 MPa for 3 min in order to form green pellets. The pellets were sintered at 390–530°C for 2 h with a heating rate of 5°C/min and then furnace cooled. The density of the sintered pellet was measured by Archimedes method. The thermal expansion coefficient of the sintered specimens was measured using a dilatometer (DIL 402 C, Netzsch, Germany). The dielectric characteristics of the sintered specimens were analyzed using an impedance gain phase analyzer (HP-4194A, USA) at 1 MHz.

Results and discussion

X-ray diffraction patterns of the xBi_2O_3–xZnO–$(1-2x)B_2O_3$ glass systems are shown in Fig. 1. The large broad peak around $2\theta = 28°$, which is a typical feature of borate glasses was observed in all compositions [13]. When $x = 0.15$, a phase separation occurred due to an immiscibility in the melt which resulted in an opaque glass [14–15]. Backscattered electron image observation as shown in Fig. 2 also supported the phase separation phenomenon and the composition of $x = 0.15$ will not considered for further examination.

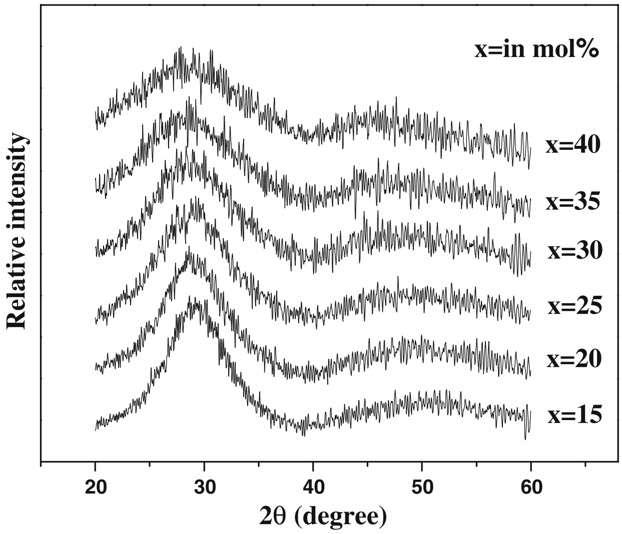

Fig. 1 XRD results of quenched compositions after melting at 1,100°C

To investigate the structure of Bi_2O_3–ZnO–B_2O_3 glass, the ^{11}B MAS-NMR spectra of the glasses were analyzed by Solid-State NMR Spectrometer. Figure 3 shows the ^{11}B MAS-NMR spectra, the proportion of N_4, and chemical shifts of BO_3 and BO_4 peaks as a function of the x (in mole%) in a xBi_2O_3–xZnO–$(1-2x)B_2O_3$ glass system. In all of the glasses, two

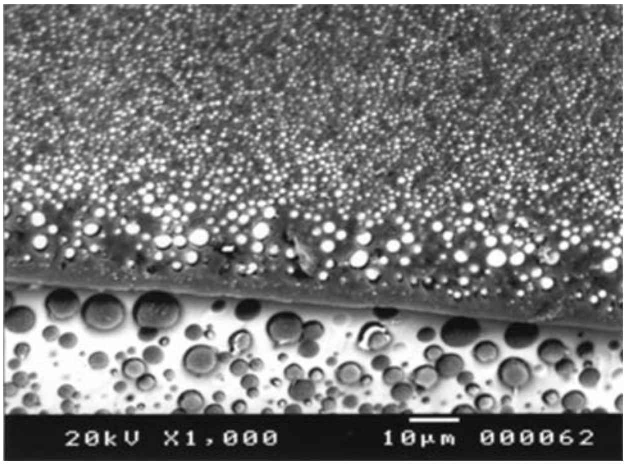

Fig. 2 BEI micrograph of the glass ($x = 15$ mol%) after quenching

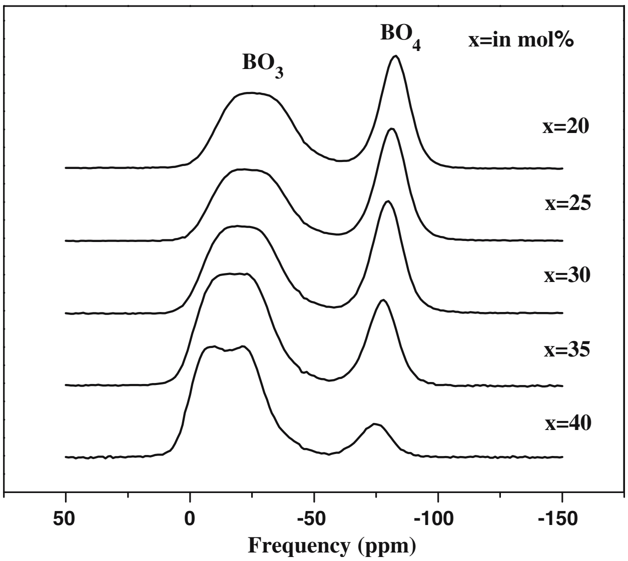

Fig. 3 ^{11}B MAS-NMR spectra as a function of *x* content (in mol%) for the studied glass samples

well-resolved peaks were clearly observed between 10 to –50 ppm and –60 to –100 ppm, which can be typically observed for most borate and borosilicate glasses [15]. The broader peak near 10 to –50 ppm originated from the trigonal boron (BO_3), and the sharp peak near –60 to –100 ppm is due to the tetrahedral boron (BO_4) [15]. Among the two peaks, the BO_3 peak is broader than the BO_4 peak since two different types of BO_3 structures coexist; one type consisted only of bridging oxygen (BO) in the structure and the other consisted of one or two non-bridging oxygens (NBO) in the structure [15–17].

The proportions of BO_3 and BO_4 were calculated from the integrated areas of their peaks as a function of the *x* [18]. The result is shown in Fig. 4. The proportion of BO_4 increased to the maximum value until $x = 25$ mol% and then decreased with the *x*. Below $x = 25$ mol%, the addition of Bi_2O_3 and ZnO replaced BO_3 with BO_4. However, above that point BO_4 decreased and BO_3 increased with Bi_2O_3 and ZnO. The changes in the structure between BO_3 and BO_4 resulting from variations of the composition are denoted as the borate anomaly. The amount of $x = 25$ mol% (totally 50 mol% of Bi_2O_3 and ZnO) in which the maximum proportion of BO_4 observed was higher than 40 mol% in the alkali borate glass and similar to 50 mol% in the intermediate oxide (PbO, SnO, CdO, and ZnO) glasses [6, 8–12]. It was also observed that with the increase of *x* both the BO_3 and BO_4 peaks shifted to a high frequency as shown in Fig. 3. The chemical shifts ranged from –25 to –15 ppm for BO_3 and from –82 to –75 ppm for BO_4. Similar chemical shifts were observed for other borate glasses, suggesting the formation of NBO [19]. The change in the proportions of BO_3 and BO_4 suggests that the Bi_2O_3 played the role of a network modifier like alkaline metals. Therefore, the units of BO_4 and BO_3 with a B–O–Bi bond are presumed to be formed. In this case, an oxygen in B–O–Bi bond might be regarded as the non-bridge oxygen since Bi_2O_3 has a much weaker bond strength of Bi–O than that of B–O in B_2O_3.

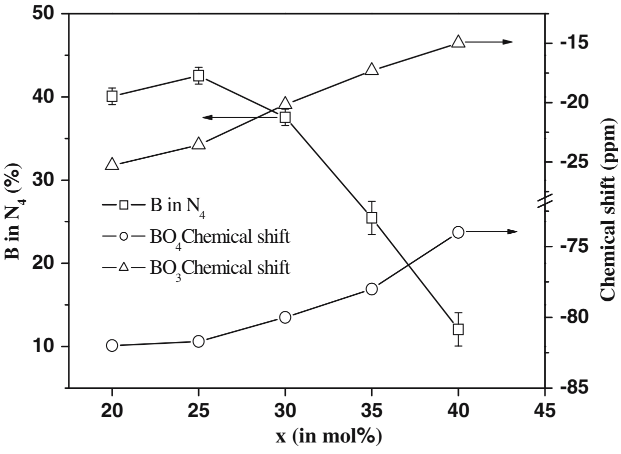

Fig. 4 The proportion of N_4 and BO_3, BO_4 chemical shift as function of *x* content (in mol%) in the Bi_2O_3–B_2O_3–ZnO glass system

If the addition of Bi_2O_3 and ZnO until $x = 25$ mol% is used for the formation of BO_4 with bridging oxygen instead of that of BO_4 with non-bridging oxygen and BO_3 with non-bridging oxygen, the glass transition temperature will increase with the increase of BO_4. However, the glass transition temperature continuously decreases with the addition of Bi_2O_3 and ZnO. This suggests the formation of BO_4 and BO_3 with non-bridging oxygen above $x = 20$ mol%. This is clearly evident in Fig. 3 (bottom), which shows chemical shifts of BO_3 and BO_4 with the addition of Bi_2O_3 and ZnO.

Figure 5 shows the glass transition temperature (T_g) as a function of the *x*. The T_g linearly decreased from 467.0 to 360.7°C as the *x* increased from 20 to 40 mol%. Generally, the T_g of glass decreases when the fraction of NBO increases because it leads to a decrease of viscosity [14]. The decrease in T_g indicates that the increase of Bi_2O_3 and ZnO above $x = 20$ mol% gives rise to the increase of NBO.

The relative densities of the sintered specimens for different *x* as a function of temperature are shown in Fig. 6. The relative density is calculated from the ratio of the sintered body density to the power density considered as theoretical density. The addition of Bi_2O_3–ZnO increased the relative density. The optimum sintering temperature, at which the maximum relative density was obtained, decreased from 520°C at $x = 20$ mol% to 420°C at $x = 40$ mol%. The maximum

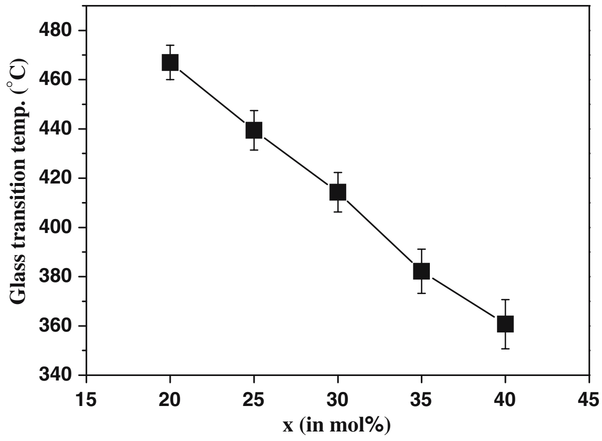

Fig. 5 Glass transition temperature (T_g) as a function of x content (in mol%)

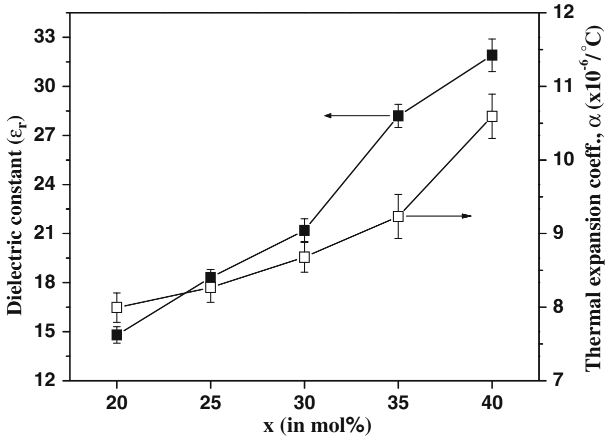

Fig. 7 Dielectric constant (ε_r) and thermal expansion coefficient (α) of glasses as a function of x content (in mol%) after optimum sintering

densification of the glass was obtained 50–60°C higher than the glass transition temperature.

Figure 7 shows the dielectric constant, ε_r and the thermal expansion coefficient, α of the samples sintered at the optimum densification temperature. As the amount of Bi_2O_3 and ZnO increased, the dielectric constant gradually increased from $\varepsilon_r = 15$ to $\varepsilon_r = 32$ and the thermal expansion coefficient increased from 7.9×10^{-6}/°C to 10.5×10^{-6}/°C [20]. The increase of the dielectric constant with Bi_2O_3 and ZnO resulted from the increase in the fraction of NBO and higher polarizability of Bi and Zn [21, 22]. The thermal expansion coefficient was lower than that of the B_2O_3 glass, 15×10^{-6}/°C. It is thought that the increase of the thermal expansion coefficient with Bi_2O_3 and ZnO was due to the increase of the non-harmonic lattice vibration induced by the NBO. The dielectric constant and thermal expansion coefficient can be calculated theoretically using Appen and Bresker's equation (Eq. 1) [21] and Appen's equation (Eq. 2) [23], respectively, which are as follows:

$$\varepsilon_r = \frac{1}{100}(\varepsilon_1 p_1 + \varepsilon_2 p_2 + \cdots \varepsilon_n p_n) = \frac{1}{100}\sum \varepsilon_i p_i \qquad (1)$$

$$\alpha = \frac{1}{100}(\alpha_1 p_1 + \alpha_2 p_2 + \cdots + \alpha_n p_n) = \frac{1}{100}\sum \alpha_i p_i \qquad (2)$$

where p_i represents the portion of the individual oxides in mol% and ε_i and α_i are the characteristic factors for each oxide. ε is 3–8 for B_2O_3 and –5–0 for ZnO. α is 14.4 for B_2O_3 and 5 for ZnO. The characteristic factor for Bi_2O_3 is not yet known. In this experiment, ε_r and α of Bi_2O_3 in Bi_2O_3–ZnO–B_2O_3 glass was obtained by using Eqs. 1 and 2. The calculated values of ε and α for Bi_2O_3 are 50–62 and 22.7–36, respectively. According to the calculated cation polarizability in single component oxides, the electric polarizability of Bi^{3+} is very larger than Zn^{2+} and B^{+3} [22]. Even though the polarizability of Bi ion in the glass and Bi_2O_3 single component could be different, the larger polarizability of Bi ion supports that the Bi^{3+} has a larger contribution to the dielectric constant than Zn^{2+} and B^{+3} which is consistent with the observation in this study.

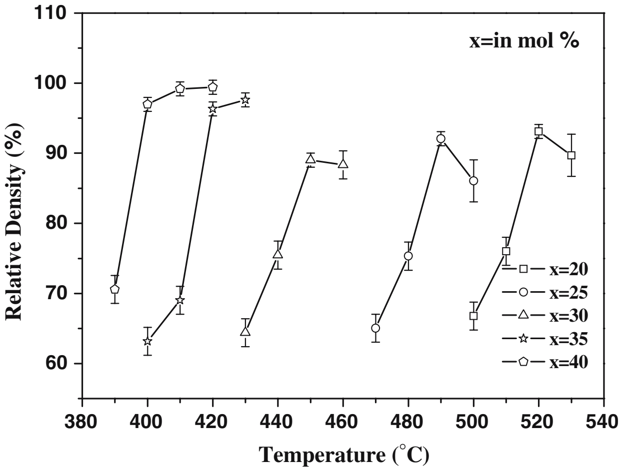

Fig. 6 Relative densities of glasses after sintering at various temperature

Conclusions

In the analysis of the ^{11}B MAS-NMR spectra for xBi_2O_3–xZnO–$(1–2x)B_2O_3$ glass, the proportion of BO_4 increased to the maximum value until $x = 25$ mol% and then decreased with Bi_2O_3 and ZnO.

However, the glass transition temperature continuously decreased with the addition of Bi_2O_3 and ZnO, suggesting the formation of BO_4 and BO_3 with non-bridging oxygen above $x = 20$ mol%. The increase of the dielectric constant with Bi_2O_3 and ZnO is attributable to the increase in the fraction of non-bridging oxygen and higher polarizability of Bi and Zn. The thermal expansion coefficient increases with Bi_2O_3 and ZnO due to the non-harmonic lattice vibration induced by the NBO. The calculated values of ε_r and α for Bi_2O_3 are 50–62 and 22.7–36, respectively.

Acknowledgement This work was supported by the National Research Laboratory grant from the Ministry of Science and Technology (MOST) and Korea Science and Engineering Foundation (KOSEF).

References

1. Scholze, Translated by Michael J. Lakin., Glass: Nature, Structure, and Properties, 3rd Ed., Springer-Verlag, New York, 1991, p 129
2. Scholze, Translated by Michael J. Lakin., Glass: Nature, Structure, and Properties, 3rd Ed., Springer-Verlag, New York, 1991, p 137
3. Warren BE, Biscoe Z (1938) J Am Ceram Soc 21:278
4. Shibata M, Sanchez C, Patel H, Feller S, Stark J, Sumcad G, Kasper J (1986) J Non-Cryst Solids 85:29
5. Chong BCL, Choo SH, Feller S, Teoh B, Mathews O, Khaw EJ, Feil D, Chong KH, Affatigato M, Bain D, Hazen K, Farooqui K (1989) J Non-Cryst Solids 109:105
6. Bray PJ, O' Keefe JG (1963) Phys Chem Glasses 4:37
7. Cha DJ (1989) Thesis, Department of Physics Graduate School, Chonnam National University, Gwangju, Korea
8. Bray PJ, Geissberger AE, Bucholts F, Harris IA (1982) J Non-Cryst Solids 52:45
9. Bray PJ, Leventhal M, Hooper HO (1963) Phys Chem Glasses 4:47
10. Hayashi A, Nakai M, Tatsumisago M, Minami T, Himei Y, Miura Y, Katada M (2002) J Non-Cryst Solids 306:227
11. Mulkern RV, Chung SJ, Bray PJ, Chryssikos GD, Turcotte DE, Risen WM (1986) J Non-Cryst Solids 85:69
12. Harris IA, Bray PJ (1984) Phys Chem Glasses 25:69
13. Lee CH, Yoo JR, Jung KW, Choi SC (2001) J Kor Ceram Soc 38:628
14. Scholze, Translated by Michael J. Lakin., Glass: Nature, Structure, and Properties, 3rd Ed., Springer-Verlag, New York, 1991, p. 162
15. Zhao P, Kroeker S, Stebbins JF (2000) J Non-Cryst Solids 276:122
16. Stebbins JF, Zhao P, Kroeker S (2000) Solid State NMR 16:9
17. Wang S, Stebbins JF (1998) J Non-Cryst Solids 231:286
18. Milberg ME, O'Keefe JG, Verhelst RA, Hooper HO (1972) J Chem Phys 13:79
19. Kroeker S, Stebbins JF (2001) Inorg Chem 40:6239
20. Boulos EN, Smith JW, Moynihan CT (1983) Glastech Ber 56:509
21. Scholze, Translated by Michael J. Lakin., Glass: Nature, Structure, and Properties, 3rd Ed., Springer-Verlag, New York, 1991, p 318
22. Dimitrov V, Sakka S (1996) J Appl Phys 79:1736
23. Scholze, Translated by Michael J. Lakin., Glass: Nature, Structure, and Properties, 3rd Ed., Springer-Verlag, New York, 1991, p 189